AN AC ELECTROSTATIC PRECIPITATOR

Bobby Elton Bennett

Thesis
Supervisor: Prof. [illegible]

May 23, 1969

AN AC ELECTROSTATIC PRECIPITATOR

by

BOBBY ELTON BENNETT
Lieutenant, United States Navy
B.S., United States Naval Academy
(1964)

Submitted to the Department of Naval Architecture and Marine Engineering in Partial Fulfillment of the Requirements of the Master of Science Degree in Electrical Engineering and the Professional Degree, Naval Engineer

at the

MASSACHUSETTS INSTITUTE OF TECHNOLOGY
May, 1969

Signature of Author.....
Department of Naval Architecture
and Marine Engineering, May 23, 1969

Certified by.....
Thesis Supervisor

Certified by.....
Reader for the Department

Accepted by.....
Chairman, Departmental Committee
on Graduate Students

AN AC ELECTROSTATIC PRECIPITATOR

by

BOBBY ELTON BENNETT

ABSTRACT

Submitted to the Department of Naval Architecture and Marine Engineering on May 23, 1969, in partial fulfillment of the requirements for the Master of Science Degree in Electrical Engineering and the Professional Degree, Naval Engineer.

One of the methods of removal of suspended particles from industrial stack gases is by electrostatic precipitation. These precipitators require a high unipolar voltage source. It is proposed to replace these unipolar potentials with 60 cps voltage. In the development of an ac electrostatic precipitator, the knowledge of precipitation times and charging times is necessary. It is with this end result in mind that precipitation experiments were made with a dc corona. One of these experiments consisted of measuring the precipitation length for varying air stream velocities to give some idea of the time to precipitate a particle once it has encountered corona. Another experiment consisted of applying positive and negative potential to spaced corona wires to determine the time required for the particle to reverse its charge and be precipitated. These times are critical when compared to the time per cycle of a 60 cps system. It was found that these times were several times shorter than the time per cycle. However, attempts at ac electrostatic precipitation were unsuccessful.

Thesis Supervisor: James R. Melcher
Title: Professor of Electrical Engineering

ACKNOWLEDGEMENTS

The author wishes to express his appreciation to Professor J. R. Melcher, Department of Electrical Engineering, Massachusetts Institute of Technology, for providing this thesis topic, and for his continued interest and guidance throughout my entire association with him. Among the other members of the Continuum Electrohydrodynamics Group who contributed both material assistance and helpful suggestions are Messrs. Harold Atlas, E. Paul Warren, and Edmund Devitt. He also wishes to thank Miss Sandra Vivolo for her efficient typing of this manuscript. A special note of thanks to my wife, Patricia, for her patience and encouragement during the preparation of this thesis.

Financial support for this research was provided by the United States Navy and the National Aeronautics and Space Administration under contract number NGL-22-009-014.

TABLE OF CONTENTS

ILLUSTRATIONS

LIST OF SYMBOLS

d	Wire to wall separation
g	Acceleration of gravity
h	Height of manometer liquid
L	Precipitate pattern length
P	Pressure
Re	Reynolds number
Rh	Hydraulic radius
S	Adjacent corona wire spacing
t, t_p	Time, Precipitation time
U	Air stream velocity
V	Voltage
v	Transverse drift velocity
W	Radians/sec
λ	Wavelength
ρ	Density
ν	Kinematic viscosity

CHAPTER I

INTRODUCTION

The removal of suspended particles from gases exhausted from industrial stacks is essential in the prevention of air pollution. The methods used to separate the particles from the gas stream can be classified into mechanical and electrical precipitators. Inertial, gravitational, and other mechanical devices act on the entire gas stream; whereas the electrical precipitator acts directly on the particles. This gives the electrostatic precipitator the ability to handle large volumes of gas, at elevated temperatures, with a reasonable small pressure drop.

The electrostatic precipitator consists of two major sections; a section for charging the particles, and a section for collecting the charged particles. The charging of the suspended particles is effected by means of a high-voltage direct-current corona usually established between a fine wire and a grounded cylindrical as in Figure 1 or plate electrode as in Figure 2. The highly concentrated electrical field at the fine wire causes the ionization of the gas. For the case where the wire is at negative polarity, the positive ions are attracted to the wire leaving negative ions

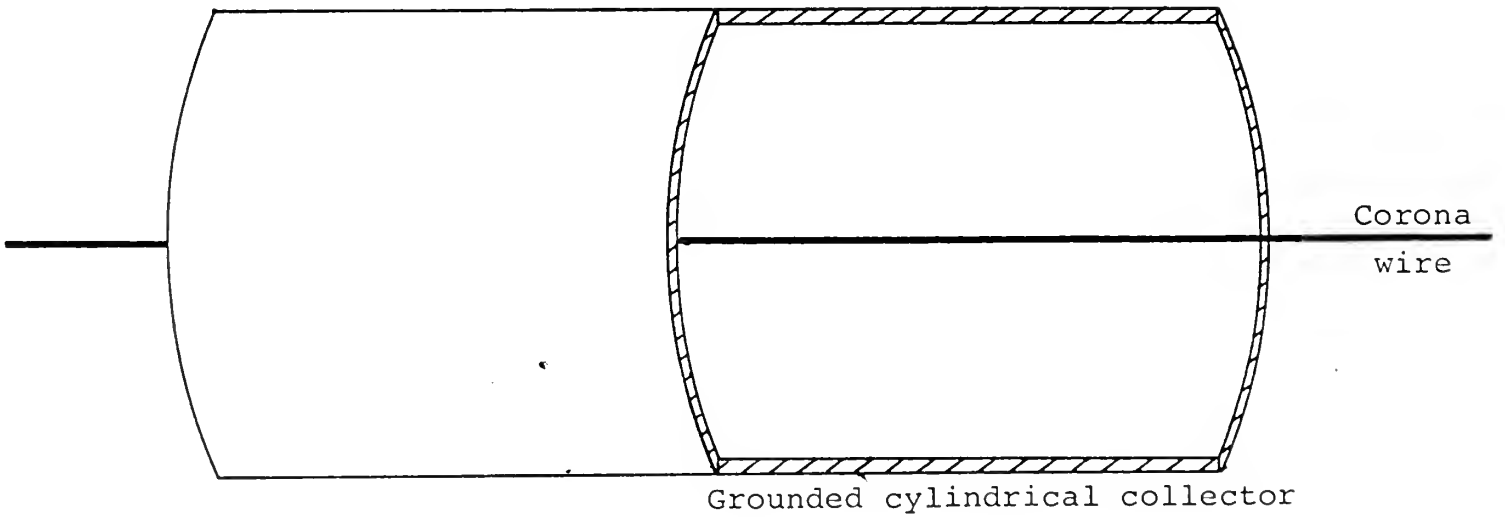

Figure 1. SCHEMATIC OF A CYLINDRICAL PRECIPITATOR

Cutaway view showing a cylindrical precipitator.

Gas flow is parallel to the corona wire.

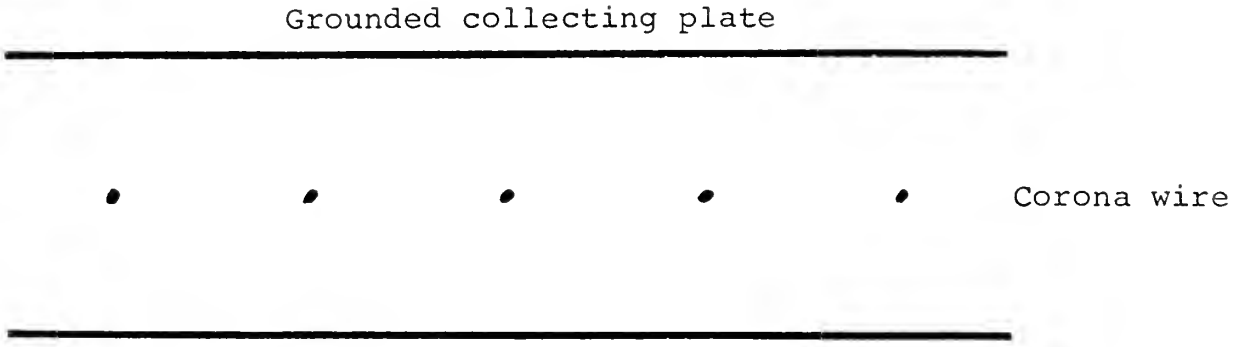

Figure 2. SCHEMATIC OF A PLATE PRECIPITATOR

In a plate precipitator, the charging and collecting sections may be separated. For the above configuration, the electric field which produces the corona also causes the particles to move to the collecting plates. The gas flow is perpendicular to the corona wires.

in most of the space between the wire and the ground electrode. The suspended particles, in passing through the corona field, are bombarded by the negative ions and become highly charged.

The collection of the particles is accomplished by having the particles attracted to an electrode by means of an unipolar field between the electrodes. The charged particles drift to the electrode, give up their charge, and adhere to the electrode. Removal can then be accomplished by mechanical rapping of the collector electrode, knocking loose the grouped particles. In many precipitators the charging and collection of the particles is performed by the same applied field.[1]

Early attempts at electrostatic precipitation were hampered by the primitive methods of producing high-voltage electrical power. The development of the synchronous-mechanical rectifier and high-voltage transformer permitted Frederick Cottrell to demonstrate the commercial feasibility of high-capacity electrostatic precipitators in 1906 at the University of California.[2] Even with the development of the high-voltage selenium rectifiers and silicon rectifiers, a major portion of the capital cost of commercial precipitators is allotted to the conversion of high-voltage alternating current power to direct current power.

Elimination of the electrical power conversion devices for electrostatic precipitators would entail either producing the proper voltages by direct current methods initially, or utilizing the alternating current produced voltages directly in the charging and collecting of the particles. It is to the latter that this thesis is addressed, the utilization of an alternating current corona to effect the precipitation of suspended particles from a gas stream.

CHAPTER II

THE AC ELECTROSTATIC PRECIPITATOR

A. Introduction

By applying a 60-cycle corona current and passing particles through the device in Figure 2, it is seen that the corona has no visible effect on the suspended particles. It was apparently self-evident to those who might have applied alternating current corona to electrostatic precipitation that the simple application above would not effect precipitation since there is no known reference to any successful work involving application of an ac corona to a precipitator.

Realizing that the obvious application of ac corona does not produce precipitation, Professor James Melcher suggested the following traveling wave precipitator. This device, which can be modeled as in Figure 3, consists of spacing the corona wires such that the 60-cycle six-phase corona source sets up a traveling ionization wave which is synchronized with the velocity of the gas stream. A particle, moving with the velocity of the gas stream, would experience a constant ionization charge during synchronization. Since some particles would be at a node of ionization, the traveling wave sections are staggered end to end to insure that all particles are collected.

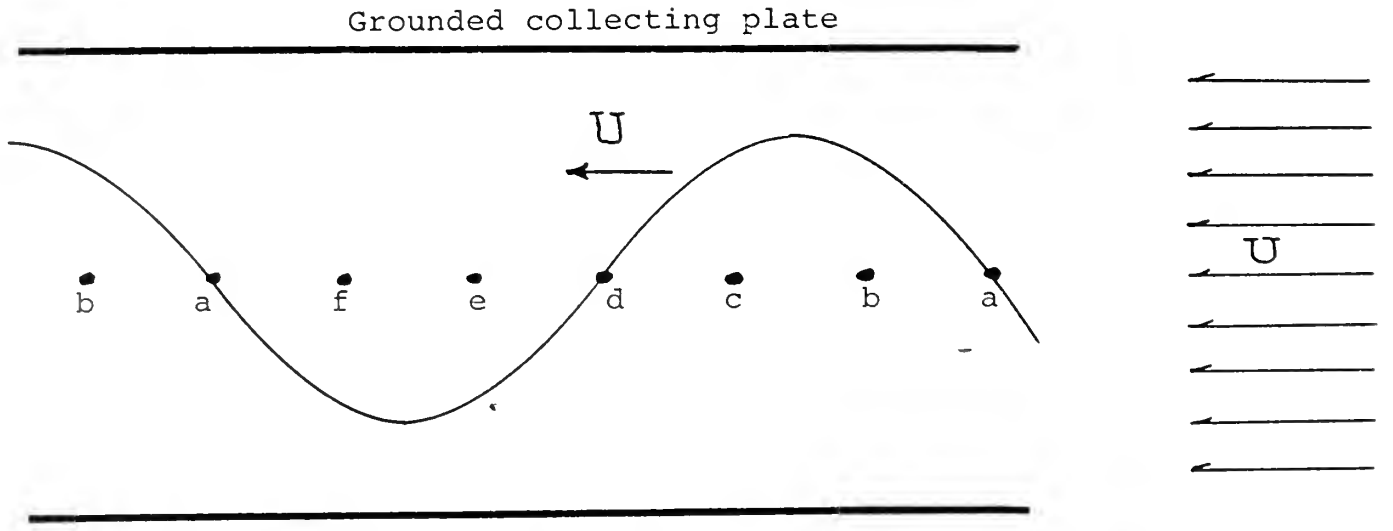

Figure 3. AC ELECTROSTATIC PRECIPITATOR CONFIGURATION

Six phase voltage source applied to corona wires a, b, c, d, e, and f creates the traveling ionization wave.

B. Determination of Gas Velocity for Synchronization

One of the factors leading to the determination of the synchronization velocity is the velocity profile of the gas stream. If the gas flow is laminar then the velocity profile is parabolic and the question arises to which velocity is the ionization traveling wave to be synchronized. This question is answered by requiring the flow to be turbulent insuring an essentially constant velocity profile. For turbulent flow, the Reynolds number is $\geq$ 5,000. For a rectangular cross section the Reynolds number is,

$$Re = \frac{4UR_h}{\nu}$$

where

$$R_h = \frac{\text{cross sectional area}}{\text{wetted perimeter}}$$

and where $\nu = 1.6 \times 10^{-4}$ ft^2/sec, the kinematic viscosity of air at atmospheric pressure and 60°F.[3] With a 1" x 2" cross section,

$$Re = 696U$$

and the flow is well into the turbulent region for velocities greater than 10 ft/sec. (Velocities typical of practical precipitators.)

The spacing of the corona wires determines the synchronization velocity. Since one wavelength, λ, of the ionization traveling wave spans six wires,

$$\lambda = 6s$$

where s is the wire to wire spacing. The traveling wire velocity is related to the wavelength and the frequency, f, through

$$U = \lambda f.$$

The wire to wire spacing is

$$s = \frac{U}{6f} = \frac{U}{360} \quad [\text{ft.}]$$

where f = 60 cycles/sec. For a velocity of 10 ft/sec, the wire spacing is .33 inch.

A lower limit can be placed on the wire to wire spacing by comparing the maximum voltage between two adjacent wires with the voltage between corona wire and grounded plate. For this six-phase system the voltage difference between adjacent wires is

$$\Delta V = V_o \sin(wt) - V_o \sin(wt-\pi/3)$$

where V_o is the maximum applied potential. Using trigonometric substitutions and simplifying, the voltage difference is found to be

$$\Delta V = V_o \cos(wt-\pi/6).$$

Interpreting this result, at some time when one wire has a potential $V_o/2$, the adjacent wire has a $-V_o/2$ potential.

This result requires that the wire to wire spacing be greater than the wire to plate spacing for proper wire to plate corona formation.

C. Wire Size Determination

The corona wire which has the largest range in voltage between corona current onset and sparkover current is considered to be the more desirable corona source. Single spring steel wires of .009, .016, .020, and .033 inches in diameter were centered between parallel conducting plates with one-inch plate separation. By measuring the plate to ground current for the corona wire voltages, the graph of Figure 4 was constructed. From this graph it is seen that the smallest diameter wire has a corona current for the largest range in voltages.

D. Description of Apparatus

The apparatus illustrated in Figure 5 is used in both ac and dc precipitation experiments. The sides of the precipitator channel consists of two 2" x 27" brass plates. The plates fit into grooves cut one inch

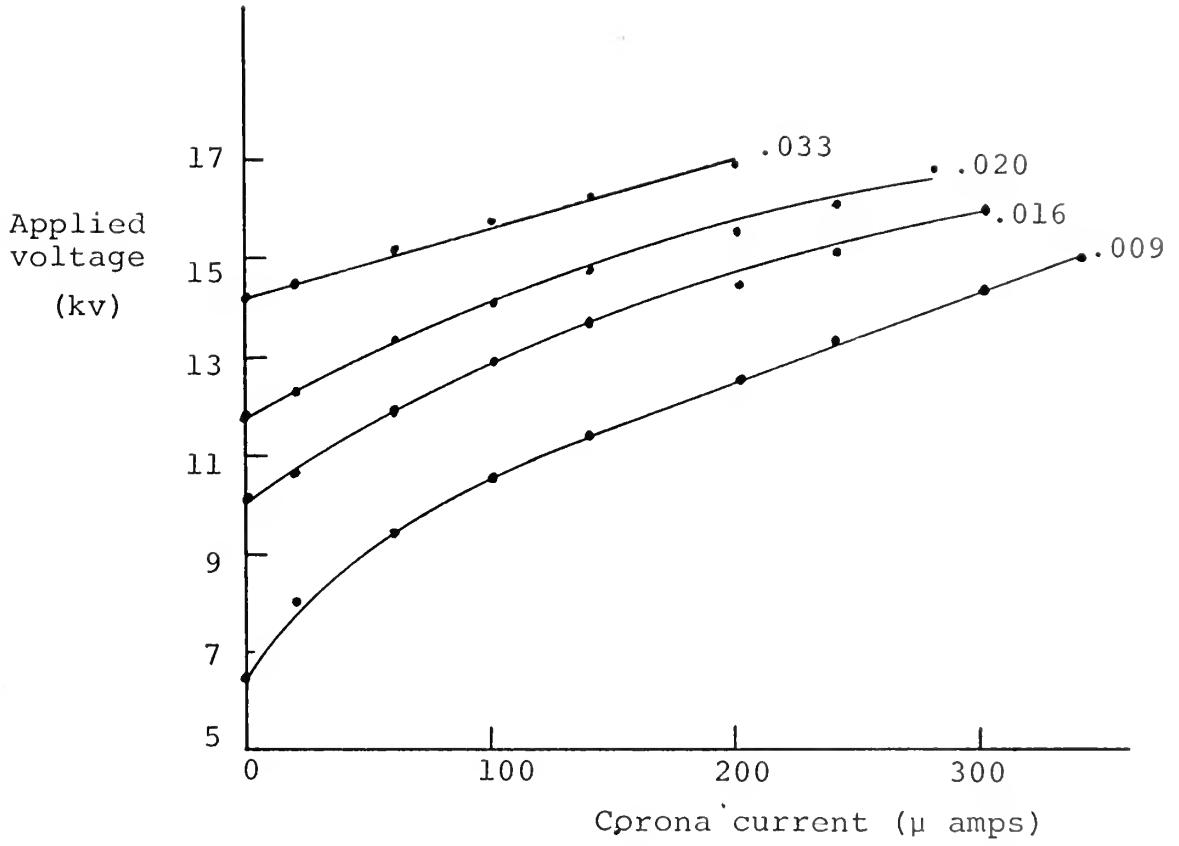

Figure 4. GRAPH OF APPLIED VOLTAGE vs. CORONA CURRENT
Spring steel vires of .009, .016, .020, and .033 inches were centered between grounded plates. The plot above shows the relationship between the voltage applied to the wire and the corona current emitted by the wire.

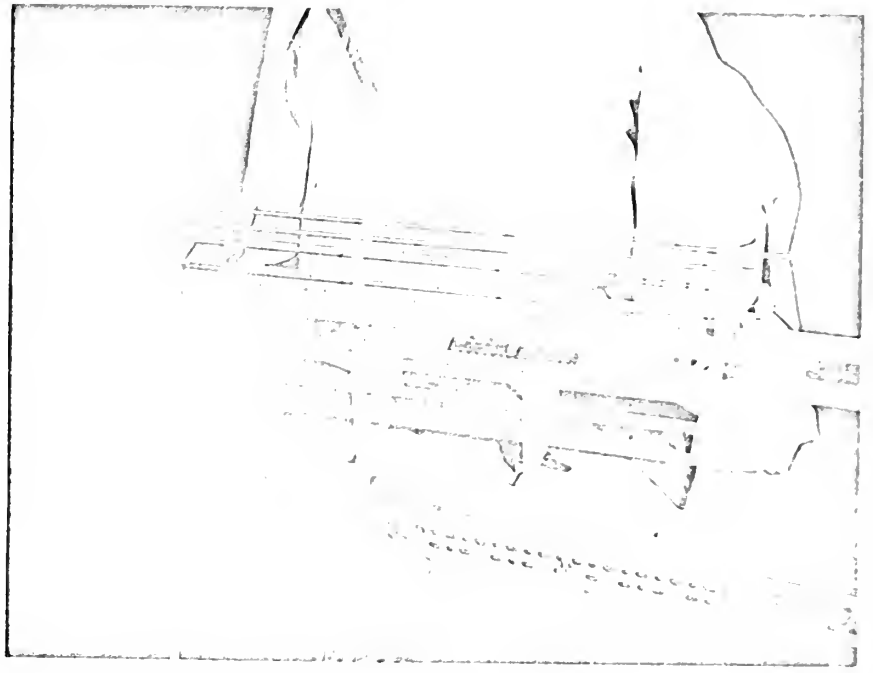

Figure 5a. PRECIPITATOR CHANNEL

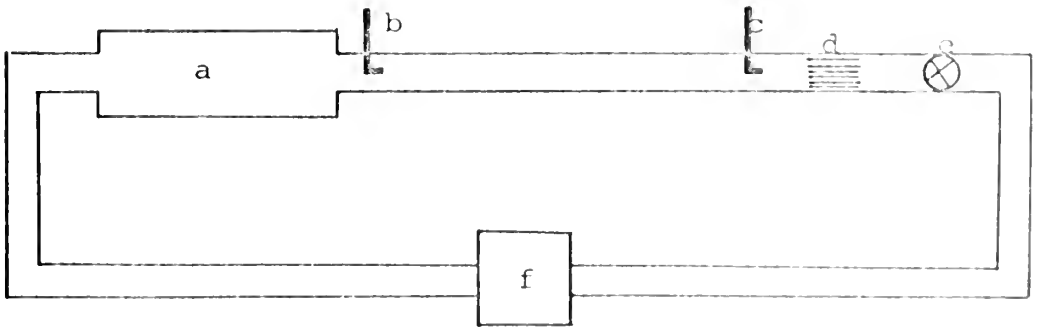

Figure 5b. SCHEMATIC OF PRECIPITATOR AND ASSOCIATED EQUIPMENT

a. Precipitator channel
b. Pitot-static tube
c. Particle injector
d. Flow straightener
e. Speed control valve
f. Fan

apart in plexiglass which forms the top and bottom of the channel. The corona wire holes in the plexiglass were drilled with 1/3-inch spacing. This setup permits synchronization velocities of multiples of 10 ft/sec by changing the wires to obtain the proper wire to wire spacing. The air stream velocity was measured by the Pitot-static tube as described in Appendix A.

The fan provides air stream velocities up to 20 ft/sec. Low pressure air is bled into the air stream to obtain velocities up to 50 ft/sec. The air stream goes through a valve, used as a throttle, before passing through an air straightener. Picking up the particles, (injection described in Appendix B), injected upstream into the flow, the air stream transverses a 42-inch entrance prior to entering the precipitator channel to ensure fully developed turbulent flow.

CHAPTER III

DISCUSSION OF EXPERIMENTAL RESULTS

A. Introduction

The precipitation experiments conducted with the apparatus described in Chapter II.D. can be grouped into two categories: those using an ac corona and those using a dc corona. The dc corona experiments consisted of:

a) applying a negative potential to the corona wires,

b) applying a positive potential to the corona wires, and

c) applying positive and negative potentials to separate groups of corona wires.

The ac corona experiments consisted of:

d) applying a single phase alternating potential to the corona wires, and

e) applying the six phase alternating potential to set up the traveling ionization wave.

The separate experiments using the positive corona and the negative corona are described as if they were the same experiment. The differences between the two coronas is attributed to the two mechanisms of ionization

production. The positive potential produces a smooth, uniform positive corona whereas the negative corona is characterized by a series of localized ionization points.[4]

For the case of the positive corona, the concentrated field near the corona wire accelerates free electrons toward the wire. With sufficient potential on the wire, the electrons attain enough kinetic energy to cause the ejection of electrons from the outer electron shell of atoms during collision. These ejected electrons continue the bombardment process. The remaining molecule is electron deficient and is a positive ion. The majority of the surrounding space consists of these positive ions drifting toward the ground electrode.

Two separate ionization mechanisms occur in the region between negative corona wire and ground electrode. The first mechanism is the electron ejection and positive ion creation by bombardment with accelerated electrons. The positive ions are accelerated to the corona wire creating additional electrons upon impact with the wire. The kinetic energy required to place electrons in the outer shells of atoms with completely filled or slightly filled outer shells is normally too high for electrons in a corona field and there is no negative corona. However, the energy required to place electrons in the outer

shell of those atoms lacking by one or two electrons a complete shell is attainable by the corona field accelerated electrons. This electron capture gives the molecule an excess of negative charge, filling most of the space as the negative ion drifts toward the ground electrode.(5)

The flue gas of industrial stacks has considerable amounts of the electronegative gases; carbon dioxide, water vapor, and oxygen. These electronegative gases render the negative corona superior to the positive corona for industrial precipitation.(6) However, during the experiments with the positive and negative corona, the only observed difference was in the precipitate patches. From Figure 6 it is seen that the negative corona leaves distinct vertically distributed patches of precipitate compared to the uniform pattern made by the positive corona. However, both have essentially the same axial distributions.

B. Unipolar Corona Precipitation

The dc corona experiments consisted of placing an unipolar potential on the corona wires, injecting the sodium bicarbonate particles, and observing the distribution of the precipitate patches. The experiments were conducted at air stream velocities of 20 and 50 ft/sec.

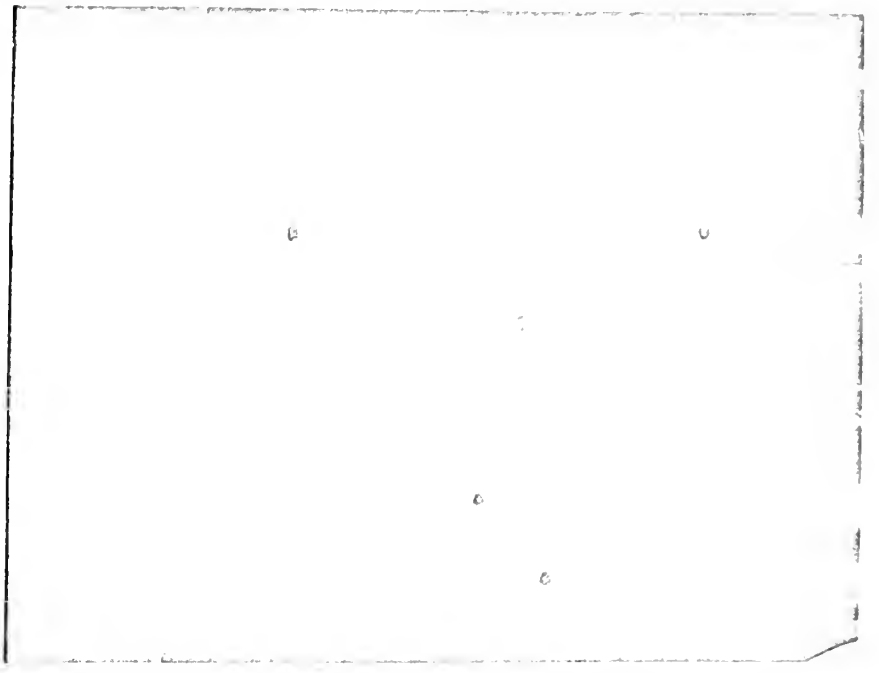

Figure 6a. NEGATIVE CORONA PRECIPITATION

U = 50 ft/sec Particle trajectory is right to left.

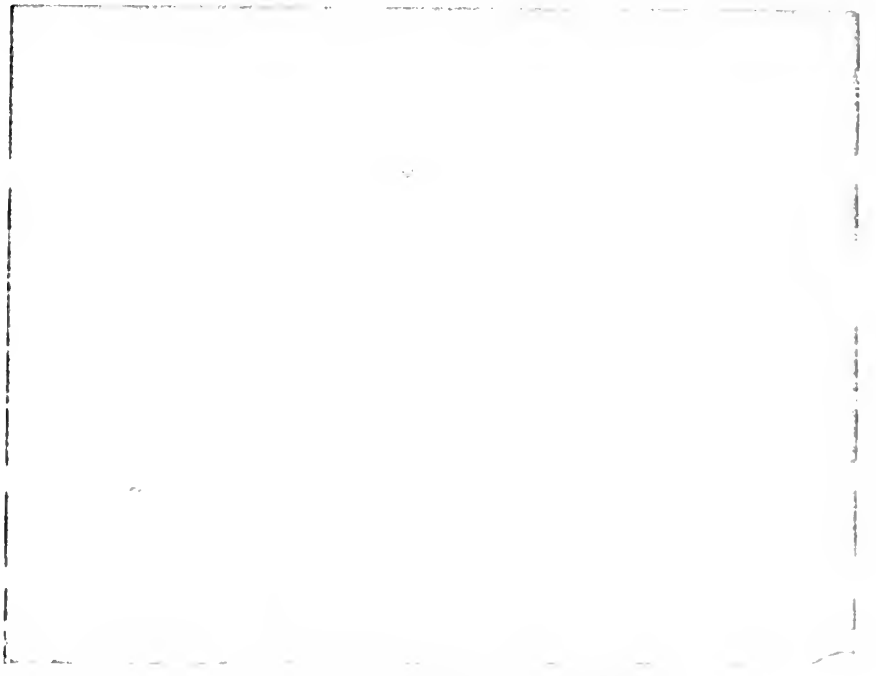

Figure 6b. POSITIVE CORONA PRECIPITATION

U = 20 ft/sec Particle trajectory is right to left.

The precipitation pattern was symmetrical, centered directly opposite the single corona wire. Even at 50 ft/sec the precipitate was observed upstream (toward the particle inlet) of the corona wire. Typical pattern lengths are tabulated in Figure 7. The density of the precipitate decreased at the pattern ends.

By placing the wires closer together, the precipitation pattern from single wires could be overlapped. However, there did not appear to be any increase in density of the precipitate over that of a single wire. This was attributed to the relative ease with which the particles could be reentrained into the air stream. An interesting side to this was observed upon clearing the plates after each experiment. The precipitate of the 20 ft/sec runs could be blown off by directing high velocity air at the plates. The precipitate of the 50 ft/sec runs required mechanical brushing to remove it from the plates.

The time, t_p, to precipitate a particle starting near the corona wire is related to the air stream velocity, U, and the precipitate pattern length, L, by the equation

$$t_p = \frac{L}{U}.$$

Air Stream Velocity U(ft/sec)	Precipitate Length L (in)	Precipitate Time $t_p = \frac{L}{U}$(sec)	Drift Velocity $v_p = \frac{d}{t_p}$ (ft/sec)
20	1.67	.007	5.95
50	1.0	.0017	24.5

Figure 7. TABLE OF PRECIPITATE PATTERN LENGTH AND PRECIPITATION TIME

Using the typical particle pattern lengths the times are

t_p = .007 sec for U = 20 ft/sec

and

t_p = .0017 sec for U = 50 ft/sec.

This analysis is based on the assumption that the particle nearest the wall is precipitated at the leading edge of the pattern and the particle nearest the corona wire is precipitated at the trailing edge.

An upper limit on the transverse drift velocity, v, can be made by using this precipitation time and the distance, d, a particle transverses to the wall from near the electrode. This relationship,

$$v = \frac{d}{t_p}$$

gives corresponding drift velocities of

v = 5.95 ft/sec for U = 20 ft/sec

and

v = 24.5 ft/sec for U = 50 ft/sec.

These drift velocities compare with the 10 ft/sec to 20 ft/sec velocities determined by White.[7]

The final dc corona experiments consisted of applying a positive potential to a group of adjacent wires upstream 1.33 inches from a group of adjacent wires with a negative potential. The experimental procedure consisted of raising the positive potential so

that 100 μamps of corona current flowed between the plate electrode and ground. After raising the negative potential so that there was no plate electrode and ground. After raising the negative potential so that there was no plate electrode to ground current, the particles were injected into the air stream. A precipitation pattern developed opposite both groups of electrodes which could not be distinguished from the patterns precipitated separately. Using the group separation of 1.33 inches (wire to wire separation) and the velocity of 20 ft/sec an upper limit on the time in which a particle is initially positively charged, neutralized, and negatively charged is .0055 sec.

C. AC Corona Precipitation

A series of precipitation runs were made by applying an alternating potential to the corona wires. The photograph of Figure 8b. was taken during one of the runs. As can be seen there was no precipitation on the conducting plates. However, the radial pattern of sodium bicarbonate on the plexiglass around the corona wires was not seen under dc operation. From the lower waveform of Figure 8a. it can be seen that there is no corona current for those portions of the applied potential waveform under the corona cutoff potential.

The six-phase alternating potentials were applied to the corona wires with .033 inch (10ft/sec) and .067 inch (20 ft/sec) spacings. The smaller spacing was abandoned due to difficulty in measuring and controlling the air stream velocity and most of all, to the facility with which adjacent corona wires tended to sparkover.

All attempts at precipitation with the .067 inch spacing were unsuccessful. The sparkover between adjacent wires had been eliminated and the 20 ft/sec air stream velocity afforded sufficient manometer height for accurate flow control. The possibility of the particles not being in synchronization still existed. The particles traveling in the coundary layer would be moving with a velocity much different from the velocity of the main flow. Even in turbulent flow the individual particles move at velocities different from the velocity of the whole.

The lack of corona current for that portion of the applied potential below corona cutoff would tend to increase the number of particles experiencing no ionization. However, the traveling ionization wave would still exist.

Figure 8a. WAVEFORM OF AC CORONA

Top waveform is that of 60 cps 5kv/cm applied potential. Bottom wave form is the resulting corona at 500 μa/cm.

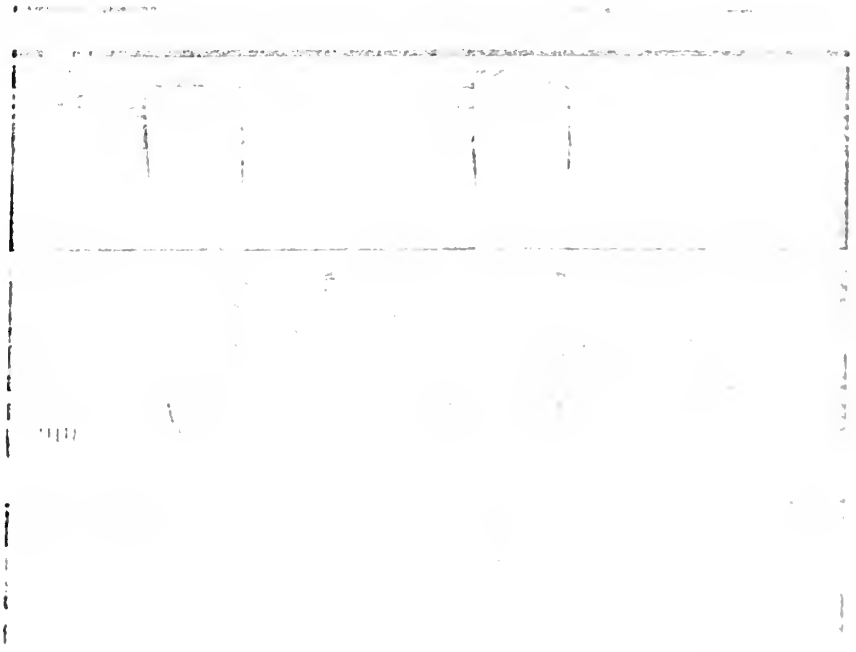

Figure 8b. PRECIPITATE [illegible]

CHAPTER IV

CONCLUSIONS

The traveling wave precipitator was not successful. In the analysis of why it was unsuccessful, all possible reasons can be reduced into the following three categories; either the particle did not experience or had insufficient time to experience unipolar ionization, or the particle was not in an unipolar collecting field for sufficient time to be precipitated, or both. These are the obvious reasons. However, it is anomalous that the traveling wave precipitation was not successful since the maximum time for charge reversal was found to be .005 sec. which is several times shorter than the .0167 sec. of a 60 cps system.

The traveling wave precipitator in this thesis should not be discarded as unworkable. It is felt that it can be made workable with more control of the variables in such a precipitator.

APPENDIX A

GAS STREAM VELOCITY MEASUREMENT AND VELOCITY PROFILE

The velocity of the air through the precipitator is determined by means of a Pitot-static tube used in connection with a manometer.

Using Bernoulli's equation for frictionless flow along a stream line,[8] then

$$P_1+\rho_a g h_1+\tfrac{1}{2}\rho_a U_1^2 = P_2+\rho_a g h_2+\tfrac{1}{2}\rho_a U_2^2 = \text{constant}$$

Here the subscripts 'a' denotes air and '1' and '2' are the points illustrated in Figure 9. At the stagnation point located at the center of the blunt nose of the probe, the velocity, U_1 is zero. For this case

$$h_1 = h_2$$

and

$$U_2 = U.$$

Solving for the velocity,

$$U = [2/\rho_a (P_1 - P_2)]^{\frac{1}{2}}$$

For the manometer illustrated in Figure 9, the pressures at points 3 and 4 are related by

$$P_3 = P_4 + \rho_f g \, \Delta h.$$

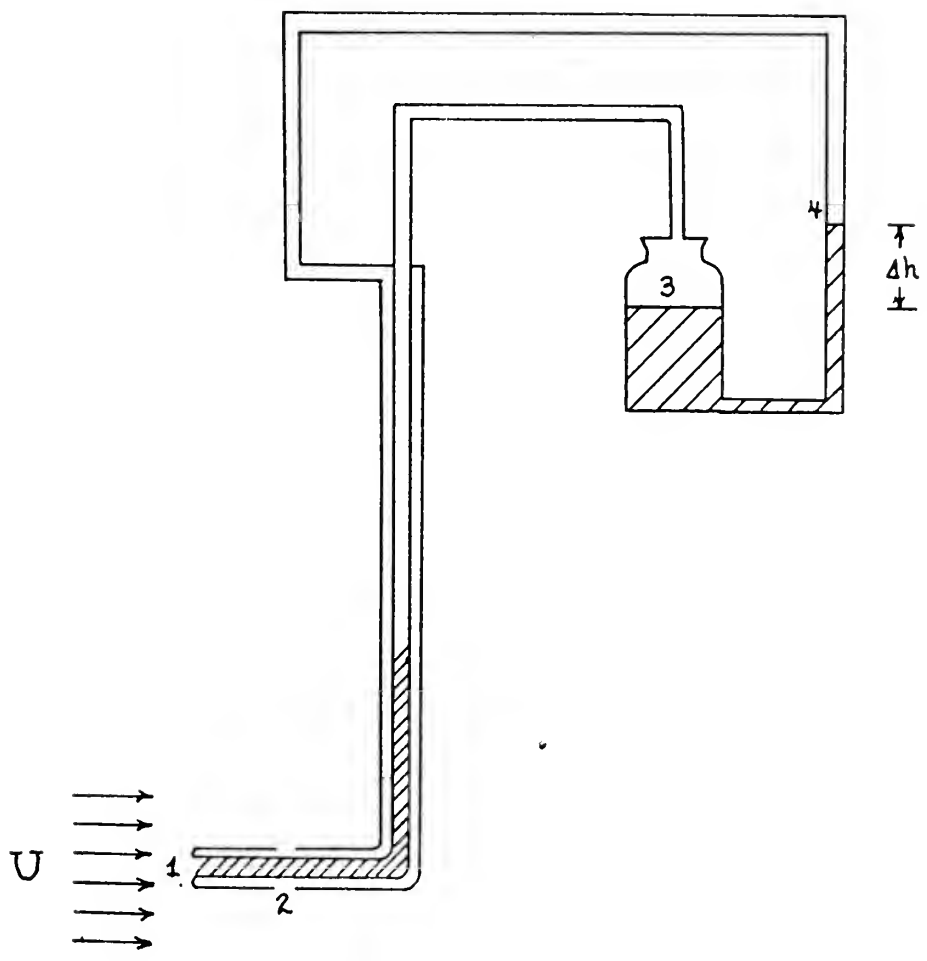

Figure 9. PITOT-STATIC TUBE AND ATTACHED MANOMETER
Point 1 is the stagnation point leading to the impact pressure area (shaded). Point 2 is at the static pressure openings.

Since

$$P_3 - P_4 = P_1 - P_2,$$

it then follows that

$$U = [2g\Delta h\ \rho_f/\rho_a]^{\frac{1}{2}}.$$

For this case where

$$\rho_a = .00237 \text{ slug/ft}^3$$

and

$$\rho_f = 1.61 \text{ slug/ft}^3,$$

then

$$U = 60.4\ (\Delta h)^{\frac{1}{2}} \quad [\text{ft/sec}]$$

where Δh is measured in inches.

The velocity profile should be essentially constant across the channel as stated in Chapter II.B. By placing the Pitot-static tube at various points, the velocity profiles in Figure 10 were obtained to substantiate the expected constant velocity.

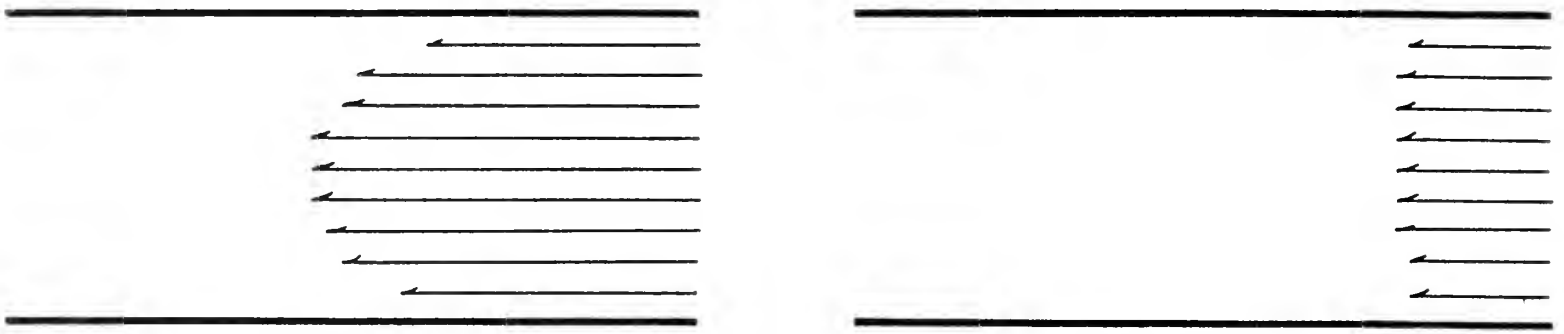

U_{max} = 50 ft/sec

U_{max} = 20 ft/sec

Figure 10. VELOCITY PROFILES (to scale)

The velocity profiles across the channel were obtained to determine whether turbulent flow was achieved. The 20 ft/sec profile was more difficult to obtain even with an inclined manometer since the manometer height has only a 0.11 inch deflection.

APPENDIX B

PARTICLE INJECTION

Of the particles (talc, fly ash, and sodium bicarbonate) readily available for laboratory experimentation, sodium bicarbonate was chosen due to its relative compatability with man. In the laboratory where the system is not completely closed, sodium bicarbonate was the least objectionable powder to other experimenters. When viewed under a microscope, the particle size is about five times as large as fly ash or talc. Sodium bicarbonate of the 50 micron particle diameter tend to coagulate.[9] To break this coagulation and disperse the particles into the passing air stream, the fluidized bed of Figure 11 was constructed.

Air at a low volumetric flow rate enters the fluidized bed causing a separation of the particles. The particles are suspended in the air acting as a fluid. The escaping air flow carries particles into the precipitator air stream.

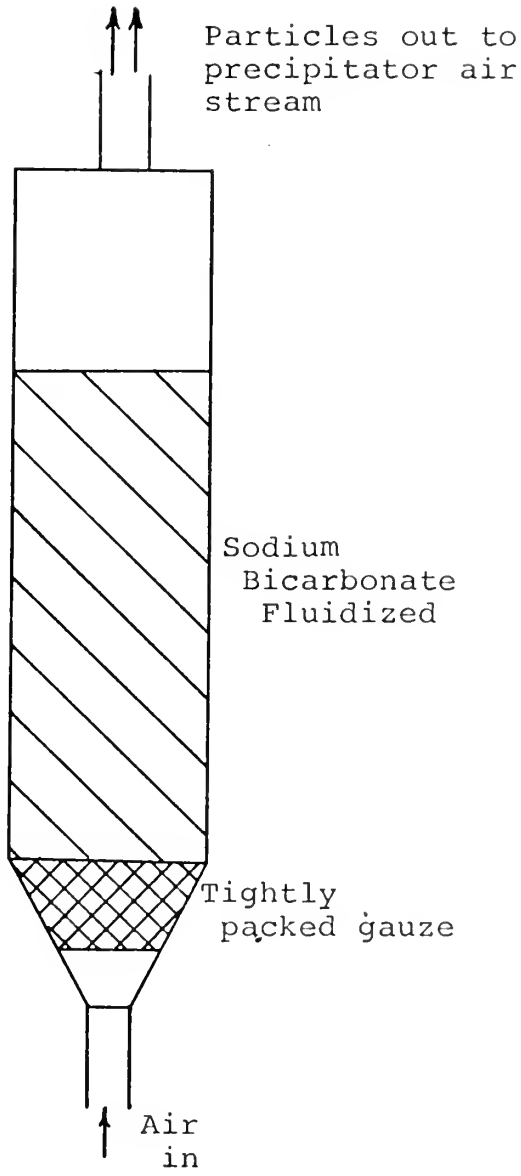

Figure 11. FLUIDIZED BED PARTICLE INJECTOR

The fluidized bed continuously furnishes a fairly uniform number of particles to the precipitator air stream.

REFERENCES

1. H. J. White, Industrial Electrostatic Precipitation. Reading: Addison-Wesley Publishing Company, Inc., 1963. PP. 1-31.

2. White, p. 6.

3. J. W. Daily and D. R. F. Harleman, Fluid Dynamics. Reading: Addison-Wesley Publishing Company, Inc., 1966. P. 35.

4. White, p. 85.

5. White, pp. 76-90.

6. White, p. 87.

7. White, p. 159.

8. Harleman, p. 129.

9. H. E. Rose and A. J. Wood, An Introduction to Electrostatic Precipitation in Theory and Practice. Second edition, London: Constable and Company LTD., 1966. P. 108.